JOURNAL OF WATER AND LAND DEVELOPMENT
e-ISSN 2083-4535

Polish Academy of Sciences (PAN), Committee on Agronomic Sciences
Institute of Technology and Life Sciences (ITP)

JOURNAL OF WATER AND LAND DEVELOPMENT
2021, No. 49 (IV–VI): 259–266; https://doi.org/10.24425/jwld.2021.137120

Available (PDF): https://www.itp.edu.pl/JWLD; http://journals.pan.pl/jwld

Received 04.06.2020
Reviewed 02.09.2020
Accepted 19.10.2020

Floodway design affected by land use changes in an urbanized area

Agus SUHARYANTO ✉, Yatnanta P. DEVIA, Indradi WIJATMIKO

Universitas Brawijaya, Faculty of Engineering, Civil Engineering Department, Jl. MT Haryono 167, Malang 65145, Jawa Timur, Indonesia

For citation: Suharyanto A., Devia Y.P., Wijatmiko I. 2021. Floodway design affected by land use changes in an urbanized area. Journal of Water and Land Development. No. 49 (IV–VI) p. 259–266. DOI 10.24425/jwld.2021.137120.

Abstract

A flood occurs for many reasons, such as excessive rainfall, runoff coefficient, or an insufficient river channel capacity. The discharge flowing through the floodway depends on the maximum main river dimension that can be normalized. LU/LC changes are affected by runoff discharge, and runoff discharge is affected by the floodway design. The study discusses the effect of land use (LU) or land cover (LC) changes and the design of floodway channel dimensions in the Kali Kemuning watershed, East Java Province, Indonesia. The Nakayasu synthetic unit hydrograph has been used to analyse the runoff discharge, and the Hydrologic Engineering Center's River Analysis System software analysed the hydraulic properties of river and floodway channels. Results show that the floodway channel design is determined by LU/LC conditions, and the river channel is normalized toward its maximum dimensions. Normalized channel depths and widths vary from 4 to 7 m and 16 to 46 m, respectively. The floodway channel is rectangular, with a bottom width of 10 m and depth of 4.5 m. With the runoff coefficient equal to 0.75, these normalized channel and floodway dimensions are suitable for the flood up to the 100-year return period runoff discharge.

Key words: *channel dimensions, channel normalization, floodway, land cover changes, land use, runoff coefficient*

INTRODUCTION

Every year, the Sampang City, East Java Province, Indonesia, is inundated with by floods caused by the overflow from the Kali Kemuning River, particularly in the rainy season. Floods analyzed occurred from 1991 to 2021 [BPBD 2020; HARYANI *et al.* 2012]. The biggest flood was on April 4th, 1993 with discharge equal to 366.4 $m^3 \cdot s^{-1}$ and the water depth at the AWLR was 9.25 m. The last flood this year occurred on January 11th, 2021 with discharge equal to 150.52 $m^3 \cdot s^{-1}$ and the water depth of 4.8 m at the AWLR. Multiple efforts have been undertaken to minimize floods, including the watershed management in the upstream area, increase in the capacity of the river channel, and the lining of the river. However, none of these methods were efficient in controlling floods. The failure of these methods was indicated by the flood that occurred on April 9th, 2020. Depending on local conditions, the use of floodways is proposed to control flooding. The design of a floodway depends on the runoff discharge. An important parameter in the runoff discharge analysis is the runoff coefficient. It depends on the land use (LU) or land cover (LC) conditions. LU/LC conditions may change every year depending on human activity and this affects the runoff coefficient. Therefore, this paper discusses the effect of LU/LC changes on the runoff discharge and influence on the floodway design.

A way to control floods in urbanized areas is to use floodways [FEMA 2018]. There are some negative effects of using a floodway, e.g. increased erosion and sedimentation, civil structure damage, and loss of the floodplain habitat. Although floodways have many negative effects detrimental to the environment, based on the feasibility study by Brantas River Basin Development Agency, East Java Province (Balai Besar Wilayah Sungai Brantas Provinsi Jawa Timur), the floodway has more advantages comparing with flood damage occurred every year at the Sampang City [BBWS 2018]. Therefore, in this case, a decision was made to use a floodway to control floods in the Sampang City. Design of a floodway is based on a number of parameters, e.g. the runoff discharge. The most important factor for the runoff discharge analysis is the runoff coeffi-

cient [BAIAMONTE 2019; LALLAM *et al*. 2018; RADECKI-PAWLIK *et al.* 2014]. The value of the runoff coefficient depends on LU/LC conditions. Therefore, the LU/LC change should be considered while designing floodways. Floodways are artificial water channels that lead midstream or downstream water to a river or an ocean in order to decrease the water flow rate [River Bureau 2007]. The volume of discharge that should flow through floodways depends on the required reduction in discharge flowing through the main channel. The safe level of discharge in the main channel is a function of runoff discharge and channel capacity. The runoff discharge depends on the rainfall intensity, runoff coefficient, topographic conditions, and watershed areas [MOE *et al*. 2017], whereas the runoff coefficient depends on LU or LC conditions [INFANZON *et al*. 2017]. Therefore, the floodway design also depends on LU/LC conditions. To design safe floodways to control floods, the main consideration should be predicted LU/LC changes. LU/LC changes that affect runoff analysis is an up-to-date topic in hydrological research [BHAGABATI, KAWASAKI 2017; JOORABIAN *et al*. 2017; GHAZAVI *et al*. 2019]. A hydrologic model is often used in the research of LU/LC impacts on runoff and sediment yield [DINKA, CHAKA 2019; KATEB *et al.* 2019; NDULUE *et al*. 2015]. Moreover, satellite images are very useful for analysing LU/LC changes [PRAKASH, SREEDEVI 2017; SIERRA-SOLER *et al.* 2015]. The runoff is analysed from the point of view of LU/LC changes and its results are used as input data to design a floodway. To reduce the occurrence of floods, floodways are the most common solution [FEMA 2016; IKEUCHI 2012; TAKEUCHI 2002].

MATERIALS AND METHODS

The study area focuses on the catchment of the Kali Kemuning River, the main river flowing through the Sampang City. Geographically, the Kali Kemuning watershed is located between 06°59′06″ S and 07°13′04″ S and 113°12′42″ E and 113°20′28″ E. The topographic map used in this research was in the scale of 1:25,000 with 12.5-m contour interval. Moreover, sixteen sheets of topographic maps were also used to analyse the river network, watershed boundary, Thiessen polygon, and other physical characteristics of watersheds. To generate the LU/LC map, the study used SPOT (Fr. Satellite Pour l'Observation de la Terre, Eng. Satellite for Observation of Earth) satellite images taken in 2008 and 2018. The city planning map of Sampang (2012–2032) was used to analyse the future LU/LC data.

Sampang is located in the Sampang Regency of the East Java Province, Indonesia. The main Kali Kemuning River has a total length of 47.8 km and approximately 14 km of the river flows through the city. The maximum discharge that can flow through the Kali Kemuning River is about 48.1 $m^3 \cdot s^{-1}$. To increase the river capacity, channel normalization was proposed. The river bank is almost entirely occupied by houses and buildings. Therefore, the normalization of the river channel is limited. The floodway dimension plan depends on the amount of reduction required in the discharge flowing through the Kali Kemuning River. The maximum discharge flow through the Kali Kemuning River depends on whether the maximum channel dimension can be normalized. The runoff discharge depends on many parameters, an important one being LU/LC, which determine the runoff coefficient. The latter is an important input to the runoff analysis. The runoff coefficient changes with LU/LC conditions. Therefore, floodway dimensions depend on the data regarding LU/LC changes, and the data are applied to the floodway design to reduce the occurrence of floods in the Sampang City caused by the Kali Kemuning River. LU/LC changes are analysed using remote sensing satellite imageries, whereas predicted river water levels are analysed using the Hydrologic Engineering Center's River Analysis System (HEC-RAS) software.

Designing a floodway requires data regarding (i) total runoff discharge, (ii) maximum flow discharge that can flow in the main channel, and (iii) amount by which that discharge should be decreased to avoid the overtopping flow. The maximum flow discharge from the watershed entering the channel is analysed using the Nakayasu Synthetic Unit Hydrograph (SUH) with input data on rainfall intensity with a return period of 2, 5, 10, 25, 50, and 100 years and analysed using the maximum daily rainfall data. The Nakayasu SUH corresponds to Equations (1)–(5) [KUSUMASTUTI *et al*. 2019]:

$$Q_p = \frac{C \cdot A \cdot R_o}{3.6(0.3T_p + T_{0.3})} \quad (1)$$

$$Q_a = Q_p \left(\frac{t}{T_p}\right)^{2.4} \quad (2)$$

$$T_{0.3} = \alpha t_g \quad (3)$$

$$\alpha = \frac{0.47(A \cdot L)^{0.25}}{t_g} \quad (4)$$

$$T_p = t_g + 0.8t_r \quad (5)$$

if $L < 15$ km, then $t_g = 0.21L^{0.7}$

if $L > 15$ km, then $t_g = 0.4 + 0.058L$

where: t = time (h), Q_p = peak discharge ($m^3 \cdot s^{-1}$), C = the surface runoff coefficient, A = watershed area (km^2), R_o = rainfall unit (mm), T_p = time to peak (h), which is the time from rain start until the peak of discharge, $T_{0.3}$ = time needed to decrease from the maximum peak discharge to 30% of the peak discharge, Q_a = rising-limb discharge ($m^3 \cdot s^{-1}$), L = the channel length (km), t_g = time concentration, t_r = flood unit time (h), t_r is $0.5t_g$ to t_g (h) that depend on the rainfall data interval, α = hydrograph parameter.

The data on the average rainfall intensity in the watershed are analysed using Thiessen polygons [ŞEN 1998]. The rainfall intensity with a certain return period is calculated based on relevant statistical formulas owing to the data distribution pattern, such as Gumbel, Poisson, and log-Pearson type III (LP3) [AL-HOURI *et al*. 2014]. The runoff coefficient depends on the percentage of the impervious area in the watershed: the higher the percentage, the higher the runoff coefficient [DAHDOUH, OUERDACHI 2018]. The runoff coefficient is analysed based on an LU/LC map generated from remote sensing satellite im-

ages and the unsupervised classification method. The value of the runoff coefficient for each LC/LU was calculated based on Table 1 [TSUTSUMI *et al.* 2004]. Having obtained the rainfall data, the next step is to consider the water level in the river. For this purpose, the HEC-RAS software is used. As already mentioned, daily rainfall data are used to analyse the rainfall intensity as input data in the simulation, whereas the HEC-RAS software uses hourly data as its input data. Therefore, it is necessary to transform daily rainfall data into hourly rainfall data, for which we use the Mononobe formula as shown in Equation (6) [NA, YOO 2018]:

$$R_t = \frac{R_{24}}{T}\left(\frac{T}{t}\right)^{2/3} \tag{6}$$

where: R_t = hourly rainfall intensity (mm·h^{-1}), R_{24} = daily rainfall intensity (mm·h^{-1}), T = rainfall duration (equal to 24 h for daily rainfall), and t = actual rainfall duration (h).

Table 1. Runoff coefficient

Type of ground surface		Runoff coefficient
Road	pavement	0.70–0.90
	permeable pavement	0.30–0.40
	gravel road	0.30–0.70
Shoulder or top of slope	fine soil	0.40–0.65
	coarse soil	0.10–0.30
	hard rock	0.70–0.85
	soft rock	0.50–0.75
Grass plot of sand	slope 0–2%	0.05–0.10
	slope 2–7%	0.10–0.15
	slope 7%	0.15–0.20
Grass plot of clay	slope 0–2%	0.13–0.17
	slope 2–7%	0.18–0.22
	slope 7%	0.25–0.35
Roof		1.00
Unused bare land		0.20–0.40
Athletic field		0.40–0.80
Park with vegetation		0.10–0.25
Mountain with gentle slope		0.3
Mountain with steep slope		0.5
A paddy field or water		0.70–0.80
Farm land		0.10–0.30

Source: TSUTSUMI *et al.* [2004], reprinted by permission of Taylor & Francis Ltd, http://www.tandfonline.com on behalf of IAHS Press.

The occurrence of floods is predicted based on water levels and bank elevation. If the water level exceeds the bank elevation, then a flood is deemed to occur.

The floodway design is analysed using the continuity formula as shown in Equation (7).

$$Q = VA_c \tag{7}$$

with the flow velocity V (m·s^{-1}) in the channel calculated using Manning's equation:

$$V = \frac{1}{n}S^{1/2}R^{2/3} \quad \text{and} \quad R = A_c/P \tag{8}$$

where: Q = discharge (m^3·s^{-1}), S = channel slope, R = hydraulic radius (m), A_c = channel cross-section area (m^2), and P = wetted perimeter (m).

The target floodway discharge depends on the amount of water to be discharged from the main channel to prevent a flood.

RESULTS AND DISCUSSION

A 1:25,000 topographic map is used to analyse the physical characteristics of the watershed. Using this topographic map, the boundary of the Kali Kemuning watershed has been analysed using the geographic information system, and the result is shown in Figure 1. Based on the river network, locations of the floodway, and the automatic water level recorder (AWLR), the Kali Kemuning River reach is divided as shown in Figure 2. The AWLR is located at Ap approximately 13.6 km from the river mouth. The runoff discharge generated from the Kali Kemuning watershed is flowing through the Kali Kemuning River. Floods have occurred in Sampang caused by the overflow of the Kali Kemuning River. The biggest flood occurred on April 4th, 1993 with the discharge of 366.4 m^3·s^{-1} and the water depth at the AWLR 9.25 m. In 2008, the floods occurred five times, i.e. on March 6th, April 21st, and November 10th, 16th, and 22nd. The 2008 hydrograph of the water level at the AWLR is shown in Figure 3. After that the flood at Sampang occurred almost every year. The flood of 2019 occurred in January 28 with the maximum discharge of 107.510 m^3·s^{-1} and water depth 4.47 m, whereas in 2021 the flood occurred on January 11th.

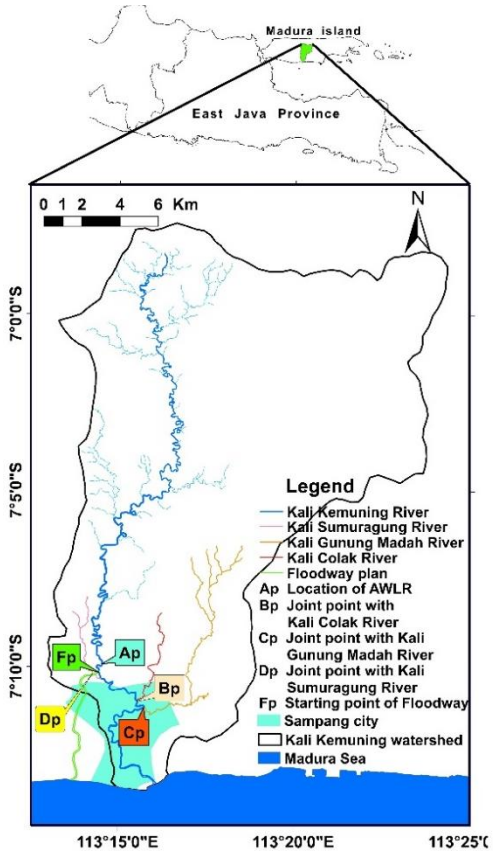

Fig. 1. Kali Kemuning watershed; source: own elaboration

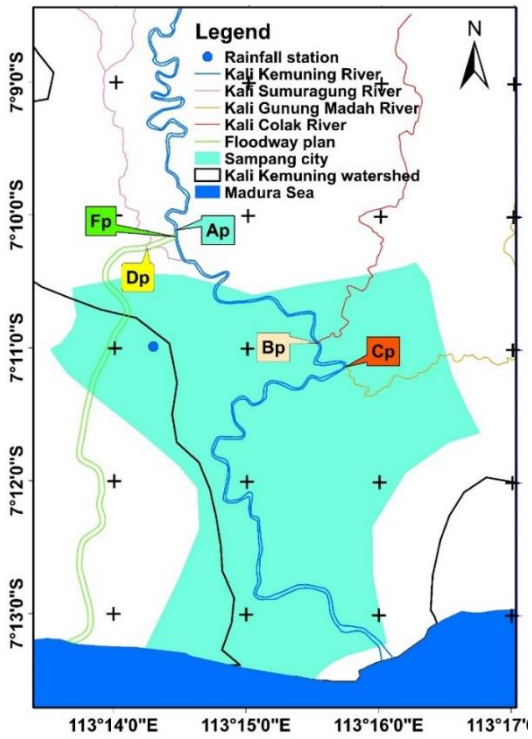

Fig. 2. Kali Kemuning River reach network; Ap, Dp, Fp as in Figure 1; source: own elaboration

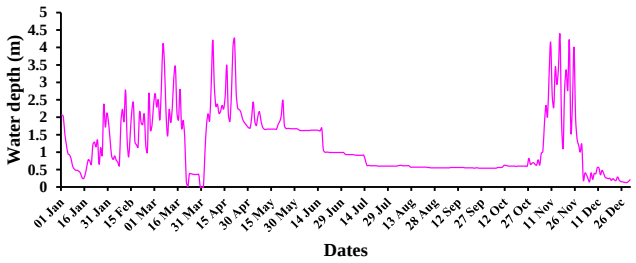

Fig. 3. Hydrograph of 2008 floods; source: BBWS Brantas Hydrologic Division [2009]

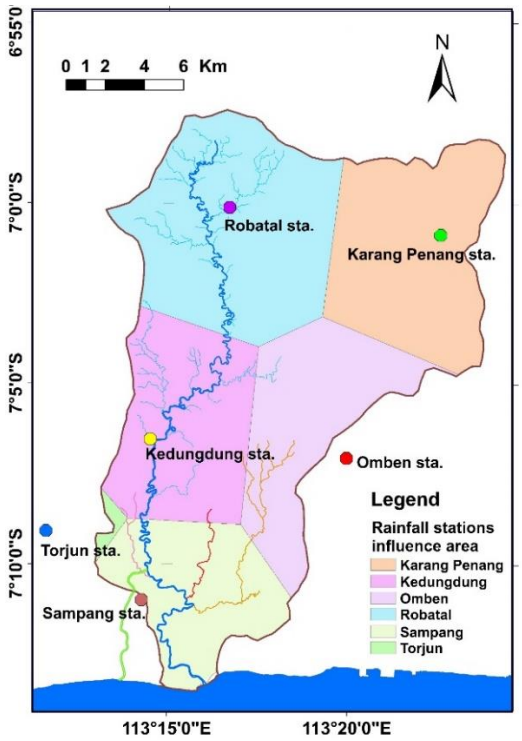

Fig. 4. Rainfall stations and Theissen polygon of the Kali Kemuning watershed; source: own study

According to the analysed results, the area of the watershed from point Ap is 317.5 km^2 with a distance of 47.8 km along the main river. Within the area from point Ap to the river mouth, there are three rivers tributaries, namely the Kali Gunung Madah River (meeting at point Bp), the Kali Colak River (meeting at point Cp), and the Kali Sumuragung River (meeting at point Dp according to the floodway plan). The floodway from the Kali Kemuning River begins at point Fp. Six rainfall stations are used to analyse the average rainfall in the watershed, namely Sampang, Torjun, Omben, Kedungdung, Robatal, and Karang Penang stations. Daily maximum rainfall data from each station in 2009–2018 have been used to analyse the rainfall intensity in the watershed.

Thiessen polygons are used to obtain the average rainfall data in the watershed for each year. The rainfall stations and the Thiessen polygon are shown in Figure 4. Owing to its statistical nature, LP3 is the most appropriate type of distribution for these data. Therefore, the LP3 formula is used to calculate the rainfall intensity in many return period years. Finally, the daily rainfall intensity with return periods of 2, 5, 10, 25, 50, and 100 years are 48, 70, 82, 100, 115, and 128 mm, respectively. The Mononobe formula is used to convert from daily to hourly rainfall data based on the 4 h rainfall duration, and the hourly rainfall data are used as the input data for analysing the runoff discharge.

The next analysis has focused the runoff coefficient. The images scanned using the HRV sensor located at the SPOT satellite in 2008 and 2018 are used to classify LU/LC changes. The unsupervised classification method is used to classify the LC. Nine LC categories are as follows: (i) forest, (ii) farm area, (iii) residential, (iv) irrigated rice field, (v) non-irrigated rice field, (vi) mangrove, (vii) salt pond, (viii) water, and (ix) salt water. From these data, the runoff coefficient is analysed as per the LC category. The LC map generated from satellite images is shown in Figure 5. This figure shows that LU/LC changed between 2008 and 2018. Due to the population growth, there are many farm areas and rice fields that changed to residential LU/LC. But some farm areas changed to forest LU/LC because of the reforestation program implemented by the Sampang Regency Government. To predict the future runoff discharge, the runoff coefficient is analysed based on the LU plan until 2032. The 2032 LU plan was designed by the local government of the Sampang Regency using the land use planning map. As shown in Table 1, the value of the runoff coefficient was calculated. Finally, the value of the runoff coefficient for 2008, 2018, and 2032 is 0.45, 0.6, and 0.75, respectively. To find the runoff discharge, the Nakayasu SUH is applied. The calculation shows eighteen peak discharges with return periods 2, 5, 10, 25, 50, and 100 years rainfall data at 2008, 2018, and 2032 runoff coefficients. There are three peak discharge data for

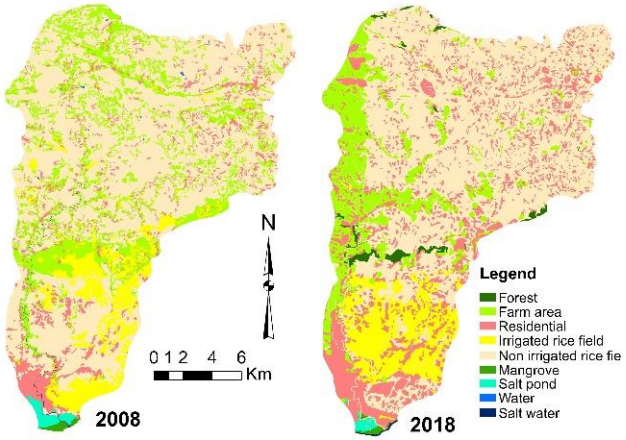

Fig. 5. Land use/land cover changes (LU/LC) map generated from satellite images; source: own study

each return period rainfall. For example, for return period of 2 years, there are three peak discharges, i.e. peak discharges for 2008, 2018, and 2032 runoff coefficients, respectively. By collating 18 peak runoff discharge data and other requirement input data, the water level in the Kali Kemuning River is analysed using the HEC-RAS software. The river cross-section and long-section data are collected from a topographical survey. The river cross-section data are collected upstream at 50-m intervals from the river mouth on a stretch of 13.6 km or until point Ap.

Based on the river reach network, as shown in Figure 2, the runoff discharges at points Ap, Bp, and Cp are calculated as follows:

$$Q_{Bp} = Q_{Ap} + Lf_{AB} + Q_{CL} \quad (9)$$

$$Q_{Cp} = Q_{Bp} + Lf_{BC} + Q_{GM} \quad (10)$$

$$Q_{Rm} = Q_{Cp} + Lf_{Cprm} \quad (11)$$

where: Q_{Ap}, Q_{Bp}, and Q_{Cp} are the runoff discharges at points Ap, Bp, and Cp respectively; Lf_{AB} is the lateral discharge from Ap to Bp, Lf_{BC} is the lateral discharge from Bp to Cp; Q_{CL} is the runoff discharge from the Kali Colak River; Q_{GM} is the runoff discharge from the Kali Gunung Madah River; Q_{Rm} is the discharge at the river mouth; and Lf_{Cprm} is the lateral discharge from Cp to the river mouth.

Q_{Ap} is used to analyse the water level in the river reach between Ap and Bp. Q_{Bp} is used similarly between Bp and Cp, and Q_{Cp} is used similarly between Cp and river mouth. Q_{Dp} is the runoff discharge at Dp, which should correspond to the flow to floodway. The analysed results for the peak discharge for each reach are given in Table 2. The 18 peak runoff discharges are used as the main input data for analysing water level profile in the river reach between Ap and the river mouth. It produces 18 water profiles for each cross-section, from which the occurrence of flood is determined. If the water level is higher than the river bank, then a flood is deemed to occur. To determine flood occurrences, runoff discharge was analysed based on *C* 2008, *C* 2018, and *C* 2032 and rainfall intensity with return periods 2, 5, 10, 25, 50, and 100 years. These runoff discharges were used as input data to the HEC-RAS software to analyse the water level profiles occurring in the Kali Kemuning River reach and in Sampang (from Ap to the river outlet). The validation of hydraulic simulation using HEC-RAS has been based on the runoff discharge when the flood occurred at Kali Kemuning River in 2008. There are five runoff data on March 6th, April 21st, and November 10th, 16th, 22nd with recorded water depths of 4.1 m, 4.25 m, 4.15 m, 4.36 m, and 4.21 m, respectively. The water depth from the HEC-RAS simulation are 3.95 m, 4.13 m, 3.95 m, 4.25 m, and 4.17 m, respectively. The agreement between water depth from simulation results and recorded at the AWLR can be found with average water depth simulation of 12.4 cm below the recorded water level. From this validation, it can be concluded that the HEC-RAS can be used for the hydraulic simulation of the Kali Kemuning River. To avoid flood, the following simulations have been performed:

1) water profile simulated using existing river dimensions; if the flood occurs, then the next scenario is undertaken;
2) water profile simulated using normalized river dimensions; if the flood still occurs, then the next scenario is undertaken;
3) water profile simulated using existing river dimensions combined with the floodway; if the flood still occurs, then the last scenario is undertaken;
4) water profile simulated using normalized river dimensions combined with the floodway; the simulation is provided by changing the floodway dimension until the flood does not occur.

Table 2. Runoff discharge in Kali Kemuning watershed

No.	Return period (y)	Discharge (Q) at different points ($m^3 \cdot s^{-1}$)						Total Q ($m^3 \cdot s^{-1}$)
		Ap	Dp	Lat. 1	Bp	Cp	Lat. 2	
1	2	192.4	32.8	21.2	20.8	39.1	33.8	307.3
2	5	280.4	48.2	30.9	30.4	57.0	49.2	447.9
3	10	338.6	57.9	37.4	36.7	68.9	59.5	541.1
4	25	412.2	70.5	45.5	44.6	83.8	72.4	658.5
5	50	466.8	79.8	51.6	50.6	94.9	82.1	745.9
6	100	521.0	89.2	57.6	56.4	106.6	91.7	832.6

Explanations: Ap, Dp, Bp, Cp as in Fig. 1; Lat. 1 = from point Ap to point Cp, Lat. 2 = from point Cp to river mouth.
Source: own study.

Table 3 summarizes the flood occurrences from the HEC-RAS simulation. If the water level at any cross-section between Ap and the river mouth is higher than the river bank then a flood is deemed to occur. As in the first simulation scenario, Table 3 shows that the Kali Kemuning River channel is not normalized and no floodway applied, then no floods occur if the rainfall intensity does not exceed the rainfall return period of 2 years and the runoff coefficient does not exceed 0.45 (runoff coefficient in 2008 LU). Because the flood still occurred, the second simulation scenario was examined. With the river channel normalized, floods occur if the rainfall intensity exceeds the rainfall return period of 5 years and the runoff coefficient exceeds 0.45. To reduce the occurrence of floods more effectively, the floodway is proposed without normalizing the river channel. This simulation is the third simulation scenario. Under those conditions, flood occurs if the rainfall return period is 100 years and *C* is 0.6 (2008 LU), as well as 25 years and *C* is 0.75 (2032 LU).

Table 3. Flood occurrence based on land use or land cover

No.	*C*	Return period (y)	Floods occur?			
			Exs.	N	Exs + Fw	N + Fw
1	0.45	2	no	no	no	no
	0.45	5	yes	no	no	no
	0.45	10	yes	yes	no	no
	0.45	25	yes	yes	no	no
	0.45	50	yes	yes	no	no
	0.45	100	yes	yes	no	no
2	0.60	2	yes	no	no	no
	0.60	5	yes	yes	no	no
	0.60	10	yes	yes	no	no
	0.60	25	yes	yes	no	no
	0.60	50	yes	yes	no	no
	0.60	100	yes	yes	yes	no
3	0.75	2	yes	no	no	no
	0.75	5	yes	yes	no	no
	0.75	10	yes	yes	no	no
	0.75	25	yes	yes	yes	no
	0.75	50	yes	yes	yes	no
	0.75	100	yes	yes	yes	no

Explanations: *C* = surface runoff coefficient, Exs. = river channel dimensions under existing conditions, N = river channel dimensions after normalization, Fw = floodway.
Source: own study.

To ensure that Sampang is free from floods, the fourth simulation scenario has been examined. Finally, if the river channel is normalized and a floodway is applied, then no floods occur when the rainfall return period is 100 years, and the runoff coefficient less than or equal to 0.75. For the existing river dimensions, Table 3 also shows that there is no flood under the 2008 LU condition if the rainfall does not exceed the rainfall with a return period of 2 years; however, floods do occur under the 2018 and 2032 LU conditions if the rainfall intensity is more than or equal to the rainfall with a return period of 2 years. This condition can be confirmed by the flood occurrence on April 9th, 2020.

To avoid the occurrence of floods, the river dimensions should be normalized, which means that the cross-section of the river should be designed to maximise the river capacity. The river channel will have its maximum capacity if the cross-section is similar to that before the sedimentation has occurred and illegal structures built on the river bank. Therefore, this condition becomes the boundary condition to increase the river dimension, particularly if the increasing river dimension requires land more than the river bank boundary. The normalized river dimensions are proposed between the Ap and the river mouth. The analysed results show that the dimensions of the Kali Kemuning River should be increased. The depth varies from 7 m at Ap to 4 m at the river mouth, and the river width varies from 16 m at Ap to 46 m at the river mouth. With these river dimensions, the river capacity at Ap to receive the runoff discharge is increased from 48.1 to 192.39 $m^3 \cdot s^{-1}$, but this capacity is only sufficient for the runoff discharge with a rainfall return period of 2 years. If the latter is 25 years, the runoff coefficient *C* is 0.75, and no floodway is used, then the water profile of this simulation (Fig. 6) shows that the water level exceeds the river bank in some places.

The water level is even higher with a rainfall return period exceeding 25 years. Therefore, it is necessary to reduce the water level below the river bank. To do so for the runoff with a rainfall return period of 25 years, the use of a floodway is proposed. To determine floodway channel dimensions, scenarios are simulated using the runoff produced at runoff coefficients 0.45, 0.60, and 0.75 with a rainfall return period of 25 years. The simulation results are summarized in Table 4. Under these conditions, the floodway channel dimensions depend on the runoff coefficient. Assuming that a floodway channel is rectangular, the channel dimensions are simulated for each value of the runoff coefficient. In general, the minimum discharge flowing through the floodway can be calculated using Equation (12):

$$Q_f = Q_{Ap} - Q_n + Q_{Dp} \tag{12}$$

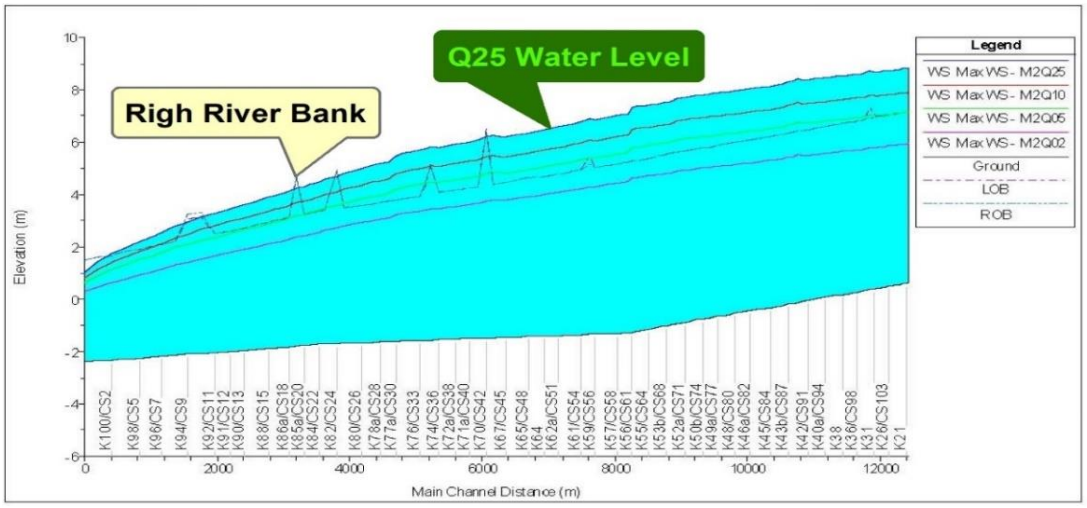

Fig. 6. Water surface profile with water discharge with return period 25 years (Q_{25}) and surface runoff coefficient (*C* = 0.75, 2032 land use conditions) normalized channel, and no floodway; source: own study

Table 4. Floodway channel dimensions for different value of runoff coefficient

No.	*C*	Maximum discharge ($m^3 \cdot s^{-1}$)				Floodway dimensions (m)	
		Ap	Kemuning River	Dp	Fp	width	depth
1	0.45	48.35	192.39	41.35	97.31	10.0	4.5
2	0.60	30.56	192.39	57.21	195.38	18.0	5.0
3	0.75	12.22	192.39	70.52	290.35	30.0	5.0

Explanations: *C* = surface runoff coefficient, Ap, Dp, Fp as in Figure 1.
Source: own study.

where: Q_f = discharge at floodway, Q_n = maximum discharge at Kali Kemuning River after normalization (192.39 $m^3 \cdot s^{-1}$), and Q_{Dp} = runoff discharge from Kali Sumuragung River. For the runoff coefficient of 0.45, the runoff discharge at Ap 247.33 $m^3 \cdot s^{-1}$ and the floodway discharge should be the runoff discharge (247.33 $m^3 \cdot s^{-1}$) minus the capacity of the Kali Kemuning River after its normalization (192.39 $m^3 \cdot s^{-1}$) plus Q_{Dp} (42.3 $m^3 \cdot s^{-1}$), namely 97.24 $m^3 \cdot s^{-1}$.

If the floodway slope is 0.0006, the Manning coefficient *n* is 0.035, and the channel is rectangular, then floodway should have a bottom width of 10 m and depth of 4.5 m. Similarly, for the runoff coefficient of 0.6, and the runoff discharge at Ap 329.77 $m^3 \cdot s^{-1}$, the required floodway discharge is 137.38 $m^3 \cdot s^{-1}$ plus the Q_{Dp} (56.4 $m^3 \cdot s^{-1}$), and the bottom width is 18 m and depth 5 m. Finally, for the runoff coefficient of 0.75, the required floodway discharge is 219.81 $m^3 \cdot s^{-1}$ plus the Q_{Dp} (70.5 $m^3 \cdot s^{-1}$), the bottom width is 30 m and the depth is 5 m. The water profile at one cross-section of the floodway is shown in Figure 7. The discharge at the river mouth is the total discharge of the Kali Kemuning watershed. It can be calculated using Equation (11). With the runoff coefficient of 0.75, the total discharge at the river mouth for rainfall return periods 2, 5, 10, 25, 50, and 100 years is given in Table 2, which shows that the discharge from point Cp to river mouth is increased. Consequently, the channel dimension is increased between Cp and the river mouth.

The present simulation results show that the LU/LC conditions have a very significant impact on the designed dimensions of the floodway channel. Therefore, it can be concluded that LU/LC changes are very important data for designing of the floodway.

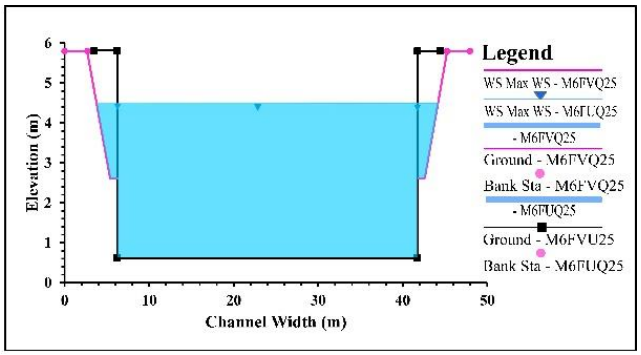

Fig. 7. Floodway channel profile; Q_{25} = 290.35 $m^3 \cdot s^{-1}$; source: own study

CONCLUSIONS

Based on the results analysed, it can be concluded that land use / land cover (LU/LC) changes in Kali Kemuning River watershed significantly affect the floodway design. LU/LC changes affect the runoff coefficient, which directly affects the runoff peak discharge. The floodway design depends on the amount of runoff discharge to be reduced from the Kali Kemuning River. Therefore, LU/LC changes must be considered crucial in floodway designs. This study has shown that the higher runoff coefficient, the larger floodway dimensions are. In case the floodway is rectangular, if the runoff coefficient equals 0.45, the floodway is 10 m in width and 4.5 m in depth. Similarly, if the runoff coefficient equals 0.60, the floodway is 18 m in width and 5 m in depth, and if the runoff coefficient equals 0.75, the floodway is 30 m in width and 5 m in depth. The social impact of the floodway development is expressed by land occupancy. The farm area and rice field lands will decrease due to the floodway construction and land property owned by citizens will decrease too.

ACKNOWLEDGMENTS

This research was supported by the Water Resources Research Group in the Civil Engineering Department, Universitas Brawijaya, Indonesia. The authors would like to thank the World Class University Programme, Universitas Brawijaya (WCUB), Faculty of Engineering through the BPPM Programme 2018 for supporting research budgets, and the BBWS Brantas for supporting research data.

REFERENCES

AL-HOURI Z., AL-OMARI A., SALEH O. 2014. Frequency analysis of annual one day maximum rainfall at Amman Zarqa Basin, Jordan. Civil and Environmental Research. Vol. 6. No. 3 p. 44–57.

BAIAMONTE G. 2019. A rational runoff coefficient for a revisited rational formula. Hydrological Sciences Journal. Vol. 65. Iss. 1 p. 112–126. DOI 10.1080/02626667.2019.1682150.

BBWS Brantas 2014. SID Pengendalian Kali Kemuning [Investigation study of Kali Kemuning River control]. Surabaya City. Brantas River Basin Development Agency East Java Province Project Report p. 84–111.

BBWS Brantas Hydrologic Division 2009. Laporan Data Muka Air Sungai Kali Kemuning Kabupaten Sampang [Water surface Data report of Kali Kemuning River Sampang Regency]. Brantas River Basin Development Agency East Java Province.

BHAGABATI S.S., KAWASAKI A. 2017. Consideration of the rainfall-runoff-inundation (RRI) model for flood mapping in a deltaic area of Myanmar. Hydrological Research Letters. Vol. 11(3) p. 155–160. DOI 10.3178/hrl.11.155.

BPBD 2020. Banjir di Sampang Madura Jawa Timur 2020 [Floods in Sampang city Madura East Java Province 2020] [online]. [Access 28.05.2020]. Available at: http://bpbd.sampangkab.go.id/category/pengumuman/

DAHDOUH Y., OUERDACHI L. 2018. Assessment of two loss methods for estimation of surface runoff in Zaafrania urban catchment, North-East of Algeria. Journal of Water and Land Development. No. 36 p. 37–43. DOI 10.2478/jwld-2018-0004.

DINKA M.O., CHAKA D.D. 2019. Analysis of land use/land cover change in Adei watershed, Central Highlands of Ethiopia.

Journal of Water and Land Development. No. 41 p. 146–153. DOI 10.2478/jwld-2019-0038.

FEMA 2016. Guidance for flood risk analysis and mapping: Hydraulics – One-dimensional analysis [online]. Guidance Document 80. Washington. DC. Federal Emergency Management Agency pp. 12. [Access 28.12.2016]. Available at: https://www.fema.gov/sites/default/files/2020-02/Hydraulics_OneDimensionalAnalyses_Nov_2016.pdf.

FEMA 2018. Guidance for flood risk analysis and mapping: General hydrologic considerations [online]. Washington. DC. Federal Emergency Management Agency pp. 20. [Access 18.04.2018]. Available at: https://www.fema.gov/sites/default/files/2020-02/General_Hydrologic_Considerations_Guidance_Feb_2019.pdf.

GHAZAVI R., SAMIE M., VALI A., PAKPARVAR M. 2019. Evaluation of the effect of land use change on runoff using supervised classified satellite data. Global NEST Journal. Vol. 21. Iss. 2 p. 245–252. DOI 10.30955/gnj.002631.

HARYANI N.S., ZUBAIDAH A., DIRGAHAYU D., YULIANTO H.F., PASARIBU J. 2012. Model Bahaya Banjir Menggunakan Data Penginderaan Jauh di Kabupaten Sampang [Flood hazard model using remote sensing data in Sampang District]. Jurnal Penginderaan Jauh. Vol. 9. No.1 p. 52–66.

IKEUCHI K. 2012. Flood management in Japan [online]. Tokyo. MLIT. [Access 20.04.2020]. Available at: https://www.mlit.go.jp/river/basic_info/english/pdf/conf_01-0.pdf.

INFAZON A.P, KENJI T, TANAKA S. 2017. Impact of land-cover change between 1990 and 2000 on the regional climate of Paraguay: A first overview. Hydrological Research Letters. Vol. 11. No. 4 p. 187–193. DOI 10.3178/hrl.11.187.

JOORABIAN S.S., SHAYESTEH K., GHOLAMALIFARD M., AZARI M., NOTIVOLI R.S., MORENO J.I.L. 2017. Impacts of future land cover and climate change on the water balance in northern Iran. Hydrological Sciences Journal. Vol. 62. Iss. 16 p. 2655–2673. DOI 10.1080/02626667.2017.1403028.

KATEB Z., BOUCHELKIA H., BENMANSOUR A., BELARBI F. 2019. Hydrological modelling using the SWAT model based on two types of data from the watershed of Beni Haroun dam, Algeria. Journal of Water and Land Development. No. 43 p. 76–89. DOI 10.2478/jwld-2019-0065.

KUSUMASTUTI C., SUDJARWO P., CHRISTHIE M., KRISNA T. 2019. Intensity-Duration-Frequency (IDF) curve and the most suitable method to determine flood peak discharge in Upper Werba Sub-Watershed. Civil Engineering Dimension. Vol. 21. No. 2 p. 70–75. DOI 10.9744/CED.21.2.70-75.

LALLAM F., MEGNOUNIF A., GHENIM A.N. 2018. Estimating the runoff coefficient using the analytic hierarchy process. Journal of Water and Land Development. No. 38 p. 67–74. DOI 10.2478/jwld-2018-0043.

MOE I.R., KURE S., JANURIYADI N.F., FARID M., UDO K., KAZAMA S., KOSHIMURA S. 2017. Future projection of flood inundation considering land-use changes and land subsidence in Jakarta, Indonesia. Hydrological Research Letters. Vol. 11. No. 2 p. 99–105. DOI 10.3178/hrl.11.99.

NA W., YOO C. 2018. Evaluation of rainfall temporal distribution models with annual maximum rainfall events in Seoul, Korea. Water. Vol. 10(10), 1468. DOI 10.3390/w10101468.

NDULUE E.L., MBAJIORGU C.C., UGWU S.N., OGWO V., OGBU K.N. 2015. Assessment of land use/cover impacts on runoff and sediment yield using hydrologic models: A review. Journal of Ecology and the Natural Environment. Vol. 7(2) p. 46–55. DOI 10.5897/JENE2014.0482.

PRAKASH C.R., SREEDEVI B. 2017. Land-use land-cover change and its impact on surface runoff using remote sensing and GIS. International Journal of Advanced Remote Sensing and GIS. Vol. 6 p. 2103–2113. DOI 10.23953/cloud.ijarsg.237.

RADECKI-PAWLIK A., WAŁĘGA A., WOJKOWSKI J., PIJANOWSKI J. 2014. Runoff formation in terms of changes in land use – Mściwojów water reservoir area. Journal of Water and Land Development. No. 23 p. 3–10. DOI 10.1515/jwld-2014-0024.

River Bureau 2007. Flood management in Japan [online]. Tokyo, Japan. MLIT. [Access 15.04.2020]. Available at: https://www.narbo.jp/data/04_materials/ma_fmij.pdf

ŞEN Z. 1998. Average areal precipitation by percentage weighted polygon method. Journal of Hydrologic Engineering. ASCE Library. Vol. 3. Iss. 1, 69. DOI 10.1061//(ASCE)1084-0699(1998)3:1(69).

SIERRA-SOLER A., ADAMOWSKI J., QI Z., SAADAT H., PINGALE S. 2015. High accuracy Land Use Land Cover (LULC) maps for detecting agricultural drought effects in rainfed agro-ecosystems in central Mexico. Journal of Water and Land Development. No. 26 p. 19–35. DOI 10.1515/jwld-2015-0014.

TAKEUCHI K. 2002. Flood management in Japan – From rivers to basins. Water International. Vol. 27 p. 20–26. DOI 10.1080/02508060208686974.

TSUTSUMI A., JINNO K., BERNDTSSON R. 2004. Surface and subsurface water balance estimation by the groundwater recharge model and a 3-D two-phase flow model. Hydrological Sciences Journal. Vol. 49. Iss. 2. DOI 10.1623/hysj.49.2.205.34837.